Feedout and Rayleigh-Taylor Seeding Induced by Long Wavelength Perturbations in Accelerated Planar Foils

R. Betti,[1,2] V. Lobatchev,[1] and R. L. McCrory[1]
[1]*Department of Mechanical Engineering, Laboratory for Laser Energetics, University of Rochester, Rochester, New York 14623*
[2]*Department of Physics, University of Rochester, Rochester, New York 14623*
(Received 14 August 1998)

The perturbation transfer between the rear and front surface (feedout), secular distortion, and Rayleigh-Taylor (R-T) instability growth is studied for long wavelength modes in accelerated flat foils. A simple formula is derived, relating the R-T growth factor to the amplitude of the rear surface perturbation. Comparisons with two-dimensional simulations confirm the validity of the theory. [S0031-9007(98)07934-4]

PACS numbers: 52.35.Py, 52.40.Nk

The Rayleigh-Taylor (R-T) instability in laser accelerated targets [1] is seeded by the laser imprinting and target nonuniformities. In recent years, the implementation of smoothing techniques [2] has produced uniform laser beams and greatly reduced laser imprinting levels in directly driven targets. Recent experimental results [3] seem to indicate that, in the near future, the level of imprinting in direct drive inertial confinement fusion (ICF) could be reduced to or below the level of target nonuniformities. The latter are particularly pronounced on the inside surface of the ICF capsules. Both direct and indirect drive ICF shells have an outer ablator and an inner layer of solid deuterium-tritium (DT) deposited on the inside surface of the ablator. The inner and outer ablator surfaces are usually very smooth while the inner DT ice surface is rough. In spite of the significant improvements in smoothing techniques [4], the DT-ice inside surface is much rougher than the ablator surface. Even though the inside surface is stable during the acceleration phase of the implosion, the nonuniformities propagate through the target and reach the ablation front (feedout [5]), thus imprinting a perturbation and seeding the ablation front R-T instability. In this paper, we describe the feedout and growth of long wavelength small perturbations in laser accelerated planar targets. We have derived a theoretical understanding of the perturbation transfer from the rear to the front surface, consequent imprinting of the perturbation and R-T seeding. Here, long wavelength small perturbations are defined as single Fourier components of the inside surface perturbations with an amplitude Δ and inverse wave number k^{-1} smaller than the postshock target thickness $d_{\rm ps}$ (i.e., linear perturbations and $kd_{\rm ps} < 1$). This theory is relevant to the stability of accelerated planar foils as well as high gain capsules [6] where the feedout process occurs well before the convergence effects become important. However, long ($kd_{\rm ps} < 1$) as well as short wavelength ($kd_{\rm ps} > 1$) feedout play an important role in seeding the R-T instability and determining the level of mixing in ignition capsules. Because of the analytic complexity, the theoretical understanding of short wavelength feedout must heavily rely on numerical simulations [7] and will be the subject of future work.

We start by determining the one-dimensional behavior of a planar foil accelerated by a large constant pressure applied on the front surface. This is a typical scenario for flat targets accelerated by a square laser pulse as well as high-gain direct drive implosion where the laser intensity (i.e., applied pressure) is initially kept constant to set the shell on the desired adiabat. We consider a planar foil of thickness d_0 and density ρ_0. At time $t = 0^-$, the outside pressure is p_0. At time $t = 0^+$, the pressure $p_a \gg p_0$ is applied on one side of the foil via laser illumination at $x = d_0$ while the pressure on the other side is kept constant at p_0. As a consequence of the sudden rise in pressure, an ionizing shock wave propagates through the foil. The shock velocity U_s depends on the shock strength and the sound speed ahead of the shock. The postshock sound speed $a_{\rm ps}$, flow velocity $U_{\rm ps}$, and gas density $\rho_{\rm ps}$ can also be expressed in terms of the shock strength and the physical properties ahead of the shock using the Hugoniot relations [8]. The target is ionized, compressed, and its thickness is $d_{\rm ps} = \rho_0 d_0/\rho_{\rm ps}$ as a result of the shock propagation. In order to simplify the analysis, we treat the compressed target material as an ideal gas with a ratio of specific heats $\gamma = 5/3$. After the shock breakout on the rear surface at time $t_{\rm sb} = d_0/U_s$, the gas expands isentropically and a rarefaction front propagates towards the front surface. The rarefaction front travels with the postshock sound speed and reaches the front surface at the rarefaction wave break-out time $t_{\rm rb} = d_{\rm ps}/a_{\rm ps}$. The rarefaction wave solution is well known and it can be easily written in the Lagrangian frame of reference defined by the initial position $\bar{x}$ of the fluid elements at the time of the shock break out. The Lagrangian transformation $(x,t) \to (\bar{x},\tau)$ can be expressed through the fluid element trajectories, $x = \bar{x} + \int_0^\tau U[\bar{x},\tau']\,d\tau'$ where $\tau = t - t_{\rm sb}$ and $0 < \bar{x} < d_{\rm ps}$. Solving the mass, momentum, and entropy conservation equations and using

 0031-9007/98/81(25)/5560(4)$15.00

the dimensionless coordinate $\xi = \bar{x}/a_{ps}\tau$ leads to the following form of the rarefaction wave solution:

$$\rho = \rho_{ps}\xi^{3/4}, \qquad p = p_{ps}\xi^{5/4}, \qquad U = 3a_{ps}(\xi^{1/4} - 1) + U_{ps}, \tag{1}$$

for $0 < \bar{x} < a_{ps}\tau$ and $\rho = \rho_{ps}$, $p = p_{ps}$, $U = U_{ps}$ for $a_{ps}\tau < \bar{x} < d_{ps}$. Here, U and U_{ps} are both negative because the shock-induced motion is directed in the negative x direction. In the target frame of reference, Eqs. (1) are equivalent to the rarefaction wave solution found in Ref. [8]. The target-vacuum interface (expansion front) travels with the escape velocity $U_{es} = U_{ps} - 3a_{ps}$ and the rarefaction front with the velocity $U_r = a_{ps} + U_{ps}$. The rarefaction wave solution is valid only until the rarefaction wave reaches the front surface. Since the applied pressure is constant, the front surface moves at constant velocity until the rarefaction wave breaks out. The front surface starts accelerating for $t \geq t_{rb}$. As shown later, it is crucial for the feedout problem and R-T growth to determine the acceleration at time $t \geq t_{rb}$. The problem can be greatly simplified by using the hodograph method in the Lagrangian frame of reference $(\bar{x}, \tau)$. The Riemann invariants $J_1 = 3a + u$ and $J_2 = 3a - u$ are constant along the characteristic curves C^+ $[d\bar{x}/d\tau = \hat{a}]$, and C^- $[d\bar{x}/d\tau = -\hat{a}]$, respectively, where $\hat{a} = a\rho/\rho_{ps}$ and $a = \sqrt{5p/3\rho}$ is the sound speed. Using the Riemann invariants as new coordinates replacing $(\bar{x}, \tau)$, the characteristic equations can be combined into a single partial differential equation,

$$\partial^2_{J_1J_2}\tau + 2[\partial_{J_1}\tau + \partial_{J_2}\tau]/(J_1 + J_2) = 0. \tag{2}$$

The solution of Eq. (2) yields the time τ as a function of the Riemann invariants: $\tau = \tau(J_1, J_2)$. Equation (2) must be solved in the domain (region II) shown in Fig. 1, between the characteristic C_0^- and the front surface $\bar{x} = d_{ps}$. In region I, $\hat{a} = \bar{x}/\tau$ and C_0^- is given by the equation $d\bar{x}/d\tau = -\bar{x}/\tau$ with initial condition $\bar{x} = d_{ps}$ for $\tau = d_{ps}/a_{ps}$. Thus, the curve C_0^- is given by $\bar{x} = d_{ps}^2/a_{ps}\tau$ and the Riemann invariants on C_0^- are $J_2 = 3a_{ps} - U_{ps}$ and $J_1 = 3a_{ps}[2\sqrt{d_{ps}/(a_{ps}\tau)} - 1] + U_{ps}$. The last equation can be inverted yielding $\tau = \tau(J_1)$ on C_0^-. The other side of region II is the front surface at $\bar{x} = d_{ps}$ where the pressure (and therefore the density and sound speed) is assigned and $J_1 + J_2 = 6a_{ps}$ is constant. Since $d\bar{x} = 0$ and $dJ_1 = -dJ_2$ on the front surface, using the characteristic equations leads to the boundary condition $\partial_{J_1}\tau + \partial_{J_2}\tau = 0$ for $\bar{x} = d_{ps}$. Using the general Riemann's solution [8] of Eq. (2) and applying the boundary conditions yield

$$T = e^{\sqrt{3}\hat{J}}[\hat{A}(\cos\hat{J} + \sqrt{3}\sin\hat{J}) - (2/\sqrt{3})\sin\hat{J}]/\hat{A}^3, \tag{3}$$

where $T = a_{ps}\tau/d_{ps}$, $\hat{A} = a/a_{ps}$, and $\hat{J} = (J_2 + U_{ps} - 3a_{ps})/(2\sqrt{3}\,a_{ps})$. The velocity u_{fs} and acceleration g_{fs} of the front surface can be obtained by substituting $\hat{A} = 1$ and $\hat{J} = -\Delta u/(2\sqrt{3}\,a_{ps})$ into Eq. (3) $(\Delta u \equiv u_{fs} - U_{ps})$ leading to the following implicit equation:

$$T = \frac{2}{\sqrt{3}}\cos\left(\frac{\Delta u}{2\sqrt{3}\,a_{ps}} + \frac{\pi}{6}\right)\exp\left(-\frac{\Delta u}{2a_{ps}}\right), \qquad g_{fs}(T) = \frac{a_{ps}}{d_{ps}}\frac{d(\Delta u)}{dT}. \tag{4}$$

The acceleration given above is valid only as long as the flow is isentropic. It is easy to show that the Jacobian of the hodograph transformation vanishes when $\tau = (9/4)(d_{ps}/a_{ps})$ at $\bar{x} = (4/9)d_{ps}$ indicating that a secondary shock forms inside the target during the acceleration phase. Thus, one can conclude that Eqs. (4) are valid until $\tau = (9/4)(d_{ps}/a_{ps})$ (or sometime after that) when the isentropic flow assumption breaks down. Since the target moves in the negative x direction, we use the transformation $x \rightarrow -x$ through the rest of this paper. At the rarefaction wave break-out time, Eq. (4) yields the front surface acceleration

$$g_{fs}(t_{rb}) = 5p_a/2\rho_0 d_0. \tag{5}$$

At later times, the front surface acceleration decreases and reaches the quasi-steady-state value $p_a/\rho_0 d_0$. This concludes the analysis of the 1D motion of the planar foil subject to a constant pressure p_a. The next step is to determine the two-dimensional evolution in the presence of a rippled rear surface.

If the rear surface is rippled, the shock-wave rippled-surface interaction produces a rippled rarefaction front [9]. We consider an initial rear surface ripple $\Delta_0\cos(ky + \pi)$. Soon after the shock breaks out on the rear surface, the ripple on the rarefaction front can be determined using the following considerations. For long wavelength modes, the motion parallel to the shock front can be neglected and the rarefaction occurs perpendicularly to the shock. As shown in Fig. 2(a), the shock first reaches the ripple valleys where the expansion and the rarefaction fronts originate. The rarefaction fan widens while the shock travels towards the ripple peaks. As shown earlier, the velocity of the rarefaction front is $U_r = a_{ps} - |U_{ps}|$. By the time the shock has reached the ripple peaks [Fig. 2(b)], the rarefaction front originated at the valleys has moved by $U_r\Delta_0/U_s$. Thus, the ripple amplitude

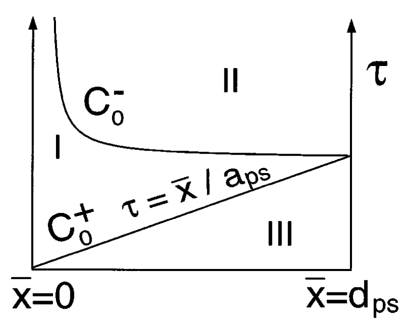

FIG. 1. Characteristics in the Lagrangian frame of reference corresponding to the shock break-out time.

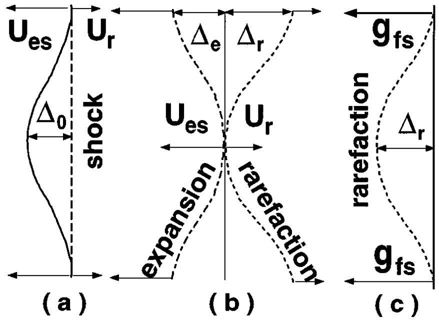

FIG. 2. The shock reaches the rippled rear surface (a); the rippled rarefaction front is formed (b); the rarefaction reaches the front (ablation) surface (c).

on the rarefaction front right after the shock has reached the peaks is $\Delta_r = \Delta_0(1 + U_r/U_s)$. The latter represents the initial conditions for the rippled rarefaction wave propagation. The peaks and valleys of the rarefaction front travel at the sound speed a_{ps} toward the front surface, thus keeping the ripple amplitude constant. Once the rippled rarefaction front approaches the front surface, the ripple valleys experience the acceleration g_{fs} before the peaks [Fig. 2(c)]. The peaks reach the front surface with a delay $\delta\tau = \Delta_r/a_{\mathrm{ps}}$. During that time, the valleys have been accelerated to the velocity $\delta v_x = g_{\mathrm{fs}}(t_{\mathrm{rb}})\delta\tau$. It follows that by the time the entire rarefaction front (peaks and valleys) has reached the front surface, a velocity perturbation is imprinted on the latter. The resulting velocity perturbation $\delta v_x \cos(ky)$ imprinted at the rarefaction wave break-out time on the front surface by the feedout process is

$$\delta v_x(t_{\mathrm{rb}}) = g_{\mathrm{fs}}(t_{\mathrm{rb}})\,(\Delta_r/a_{\mathrm{ps}})\,, \qquad (6)$$

where $g_{\mathrm{fs}}(t_{\mathrm{rb}})$ is given by Eq. (5). Moreover, the target mass under the valleys of the initial perturbation is less than under the peaks because the target thickness under the valleys is Δ_0 less than under the peaks. Since the target acceleration depends on the mass/thickness, a perturbation in the acceleration $\delta g_{\mathrm{fs}} \cos(ky)$ develops between the peaks and the valleys,

$$\delta g_{\mathrm{fs}} = -(\partial g_{\mathrm{fs}}(t)/\partial d_0)\Delta_0\,. \qquad (7)$$

where g_{fs} is given by Eq. (4) as long as the flow is isentropic. At later times ($t \gg t_{\mathrm{rb}}$), the acceleration reaches a quasi-steady-state $g_{\mathrm{fs}} \to p_a/\rho_0 d_0$ and the perturbed acceleration becomes

$$\delta g_{\mathrm{fs}} \to g_{\mathrm{fs}}(t)\Delta_0/d_0\,. \qquad (8)$$

We conclude that the feedout process of long wavelength modes leads to the imprinting of a velocity and an acceleration perturbation on the front surface. Equations (6),(7) are derived as a lowest order expansion in $kd_{\mathrm{ps}} < 1$ because any transversal motion has been neglected.

The growth of the Rayleigh-Taylor instability starts after the rarefaction wave break-out time and it is seeded by the imprinted velocity and acceleration perturbations. Only in the limit of $k \to 0$, no R-T growth occurs and the front surface distortion Δ_{fs} grows secularly because of the imprinted velocity and acceleration perturbations described by the following ordinary differential equation (ODE) and initial conditions: $[\ddot{\Delta}_{\mathrm{fs}}]_{k\to 0} = \delta g_{\mathrm{fs}}$, $\Delta_{\mathrm{fs}}(t_{\mathrm{rb}}) = 0$, $\dot{\Delta}_{\mathrm{fs}}(t_{\mathrm{rb}}) = \delta v_x(t_{\mathrm{rb}})$. Initially, the ripple is driven by the imprinted velocity perturbation and grows linearly in time. Then, the perturbed acceleration leads to a quadratic secular distortion. For finite wave numbers, the R-T instability takes over at later times and the ripple amplitude grows exponentially. Because of the complexity of the analytic solution, we rely on a simplified model and physical intuition to study the R-T growth from the imprinted perturbations. We assume that the R-T is a surface instability inducing an incompressible perturbed velocity field and neglect the effect of ablation [6] on long wavelength modes. A careful comparison with numerical simulations will determine the validity of the R-T model.

We consider an incompressible layer of thickness d_{ps} subject to the acceleration $g(t)$ in a vacuum. The linear analysis shows that the front $\Delta_{\mathrm{fs}} \cos(ky)$ and rear surface $\Delta_{\mathrm{rs}} \cos(ky)$ distortions produced by long wavelength modes can be written as

$$\begin{aligned} \Delta_{\mathrm{fs}} &= (\Delta^+ + \Delta^-) \\ \Delta_{\mathrm{rs}} &= [\Delta^+(1 - kd_{\mathrm{ps}}) + \Delta^-(1 + kd_{\mathrm{ps}})], \end{aligned} \qquad (9)$$

where Δ^+ and Δ^- represent a couple of growing/damped and oscillatory modes satisfying the following ordinary differential equations: $\ddot{\Delta}^+ = kg(t)\Delta^+$ and $\ddot{\Delta}^- = -kg(t)\Delta^-$. Four initial conditions are needed to solve the two ODEs. For the feedout problem, two initial conditions are provided by the front surface and velocity perturbations at the rarefaction wave break-out time: $\Delta_{\mathrm{fs}}(t_{\mathrm{rb}}) = 0$ and $\dot{\Delta}_{\mathrm{fs}}(t_{\mathrm{rb}}) = \delta v_x(t_{\mathrm{rb}})$. Furthermore, since the flow is incompressible, $\dot{\Delta}_{\mathrm{rs}}(t_{\mathrm{rb}}) = \dot{\Delta}_{\mathrm{fs}}(t_{\mathrm{rb}})$. The last condition is provided by assigning $\Delta_{\mathrm{rs}}(t_{\mathrm{rb}})$ in such a way that the asymptotic value of the acceleration perturbation is the same as in the real compressible problem. By setting $\Delta_{\mathrm{rs}}(t_{\mathrm{rb}}) = -\Delta_{\mathrm{ps}} = -\Delta_0 d_{\mathrm{ps}}/d_0$, the acceleration perturbation of the incompressible foil of thickness d_{ps} is $\delta g_{\mathrm{inc}} = g(t)\Delta_0/d_0$ identical to the asymptotic compressible value as shown in Eq. (8). However, during a brief transient after the rarefaction wave breaks out $\delta g \neq \delta g_{\mathrm{inc}}$. In order to correctly include the secular distortion occurring during this transient, we add a nonhomogeneous term into the equations for Δ^+ and Δ^- reproducing the exact δg and secular distortion for $k \to 0$. Our final model describing the secular distortion as well as the R-T growth can be written in the following form:

$$\ddot{\Delta}^{\pm} = \pm kg_{\mathrm{fs}}(t)\Delta^{\pm} + [\delta g_{\mathrm{fs}} - g_{\mathrm{fs}}(t)\Delta_0/d_0]/2\,, \qquad (10)$$

where g_{fs} is the front surface acceleration and $\delta g_{\mathrm{fs}} = -(\partial g_{\mathrm{fs}}/\partial d_0)\Delta_0$ is the exact perturbed acceleration. The front surface distortion is given by $\Delta_{\mathrm{fs}} = \Delta^+ + \Delta^-$.

Equations (10) must be solved using the following initial conditions:

$$\Delta^+(t_{\mathrm{rb}}) = -\Delta^-(t_{\mathrm{rb}}) = \Delta_0/2kd_0$$
$$\dot{\Delta}^+(t_{\mathrm{rb}}) = \dot{\Delta}^-(t_{\mathrm{rb}}) = \delta v_x(t_{\mathrm{rb}})/2\,, \tag{11}$$

where Δ_0 and d_0 are the initial (uncompressed) rear-surface perturbation amplitude and target thickness, respectively, and $\delta v_x(t_{\mathrm{rb}})$ is the imprinted velocity perturbation as given by Eq. (6). It is easy to show that Eqs. (10),(11) yield the correct secular distorion equation for $k \to 0$. If a steady state is reached shortly after the rarefaction wave breaks out, Eqs. (10),(11) can be solved analytically. In this case, the time asymptotic behavior $[t > t_{\mathrm{rb}} + (kg_{\mathrm{fs}})^{-1/2}]$ of the solution can be approximated by the following simple formula:

$$\Delta_{\mathrm{fs}} \approx \frac{1}{4}\left(\frac{\Delta_0}{kd_0} + \sqrt{\frac{3}{5}\frac{\rho_{\mathrm{ps}}}{\rho_0}}\frac{\Delta_r}{\sqrt{kd_0}}\right) \times \exp\left[\int_{t_{\mathrm{rb}}}^{t} \sqrt{kg_{\mathrm{fs}}(t')}\,dt'\right], \tag{12}$$

where $\Delta_r = 0.8\Delta_0$ and $\rho_{\mathrm{ps}} \simeq 4\rho_0$ for strong shocks. The WKB integral is used to improve the accuracy at shorter wavelengths and includes the early temporal changes of $g(t)$. Equation (12) represents an approximate, yet accurate, formula for the front surface distortion seeded by a rear surface perturbation of amplitude Δ_0. Observe that the R-T induced distortion depends on the wave number through the growth rate as well the coefficient of the exponential. The latter increases as k decreases. It is easy to show that the first and second terms in the coefficient are produced by the imprinted acceleration and velocity perturbations, respectively.

The accuracy of Eq. (12) and the R-T model [Eqs. (10),(11)] has been tested by comparing the analytic results with two-dimensional Lagrangian simulations of a 20 μm thick target with initial density $\rho_0 = 1\ \mathrm{g/cm^3}$ and pressure of 10 kbar accelerated by an applied constant pressure $p_a = 20$ Mbar. The initial rear surface perturbation amplitude is $\Delta_0 = 0.05\ \mu$m, the shock and rarefaction wave break-out times are $t_{\mathrm{sb}} = 0.4$ ns and $t_{\mathrm{rb}} = 0.58$ ns. Figure 3 shows the time evolution of the front surface distortion Δ_{fs} obtained from Eqs. (10),(11), the approximate formula Eq. (12), and the simulations for wavelengths $\lambda = 60\ \mu$m ($kd_{\mathrm{ps}} \simeq 0.5$) and $\lambda = 300\ \mu$m ($kd_{\mathrm{ps}} \simeq 0.1$). The functions $g_{\mathrm{fs}}(t)$ and $\delta g_{\mathrm{fs}}(t)$ are obtained from Eqs. (4),(7) while the flow is isentropic and from the 1D numerical simulations after that. Although Eqs. (4),(7) have been derived for isentropic flows (the secondary shock formation time is 0.8 ns), they can be used as long as the secondary shock is weak up to about 1.2 ns as indicated by numerical simulations.

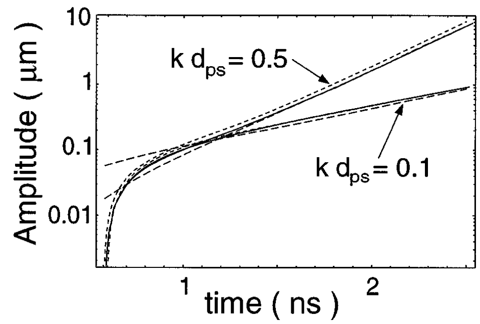

FIG. 3. Front surface distortion predicted by the simulations (solid line), the model Eqs. (10),(11) (dotted line), and Eq. (12) (dashed line) for two wavelengths. Overlapping occurs for both wavelengths.

The good agreement between analytic theory and simulations shows that Eq. (12) can indeed be used to estimate the level of distortions induced by a long wavelength rear-surface perturbation with $kd_{\mathrm{ps}} < 1$.

The authors would like to thank Dr. V. Goncharov for many useful discussions on the R-T model described in his Ph.D. thesis [10]. This work was supported by the U.S. Department of Energy under Cooperative Agreement No. DE-FC03-92SF19460.

[1] J.H. Nuckols *et al.*, Nature (London) **239**, 139 (1972).
[2] S. Skupsky *et al.*, J. Appl. Phys. **66**, 3456 (1989); R.H. Lehmberg, A.J. Schmitt, and S.E. Bodner, J. Appl. Phys. **62**, 2680 (1987).
[3] C.J. Pawley *et al.*, Phys. Plasmas **4**, 1969 (1997); A.V. Deniz *et al.*, Opt. Commun. **147**, 402 (1998); S.E. Bodner *et al.*, Phys. Plasmas **5**, 1901 (1998).
[4] J.K. Hoffer and L.R. Foreman, Phys. Rev. Lett. **60**, 1310 (1988).
[5] D.C. Wilson *et al.*, Phys. Plasmas **5**, 1953 (1998).
[6] J.D. Lindl, *Inertial Confinement Fusion* (Springer, New York, 1998), pp. 61, 156.
[7] S.A. Bel'kov *et al.*, Phys. Plasmas **5**, 2988 (1998).
[8] G.B. Whitham, *Linear and Nonlinear Waves* (Wiley, New York, 1974), pp. 167, 174, 183.
[9] Y. Yang, Q. Zhang, and D.H. Sharp, Phys. Fluids **6**, 1856–1873 (1994); A. Velikovich, Phys. Fluids **8**, 1666–1679 (1996); J.G. Wouchuk and K. Nishihara, Phys. Plasmas **3**, 3761–3776 (1996).
[10] V. Goncharov, Ph.D. thesis, University of Rochester, 1998.